Available online at www.sciencedirect.com
SCIENCE DIRECT
International Journal of Heat and Mass Transfer 49 (2006) 3349–3359
International Journal of HEAT and MASS TRANSFER
www.elsevier.com/locate/ijhmt

Fully-developed heat transfer in annuli with viscous dissipation

P.M. Coelho [a], F.T. Pinho [b,c,*]

[a] Centro de Estudos de Fenómenos de Transporte, DEMEGI, Faculdade de Engenharia, Universidade do Porto, Rua Dr. Roberto Frias s/n, 4200-465 Porto, Portugal
[b] Centro de Estudos de Fenómenos de Transporte, Faculdade de Engenharia, Universidade do Porto, Rua Dr. Roberto Frias s/n, 4200-465 Porto, Portugal
[c] Universidade do Minho, Largo do Paço, 4704-553 Braga, Portugal

Received 20 October 2005
Available online 12 June 2006

Abstract

For Newtonian concentric annular flows analytical solutions are obtained under imposed asymmetric constant wall heat fluxes as well as under imposed asymmetric constant wall temperatures, taking into account viscous dissipation and for fluid dynamic and thermally fully-developed conditions. Results for the special case of the heat flux ratio for identical wall temperatures and the critical Brinkman numbers marking changes of sign in wall heat fluxes are also derived.

Equations are presented for the Nusselt numbers at the inner and outer walls, bulk temperature and normalised temperature distribution as a function of all relevant non-dimensional numbers. Given the complexity of the derived equations, simpler exact expressions are presented for the Nusselt numbers for ease of use, with their coefficients given in tables as a function of the radius ratio.

Keywords: Annular flow; Asymmetric heating; Internal viscous dissipation; Imposed wall temperatures; Imposed wall heat fluxes

1. Introduction

A common geometry in heat exchangers is the concentric annular duct which has been the topic of countless heat transfer and fluid mechanics research, as summarized by Shah and London [24] and Kays et al. [12], amongst others. Other common industrial applications of annular flows in the laminar regime, for which this work is quite relevant, are tube extrusion of high viscosity fluids [1], cooling of electronic components and transmission cables. In spite of the effort, the literature still shows gaps of information for some conditions of operation, which we aim to reduce with this contribution. Analytical solutions, such as those obtained here, also serve as test cases for validating numerical solutions, have a pedagogical motivation and provide the simplest, most efficient way to perform parametric investigations of the effects of independent variables on output quantities.

The objective of this work is to present analytical heat transfer solutions for the annular flow of very viscous Newtonian fluids, i.e., including effects of viscous dissipation. Here, only thermally and dynamically fully-developed flow is considered and two different sets of wall boundary conditions are separately investigated: imposed heat fluxes and imposed wall temperatures. In each case the imposed conditions are peripherally and axially constant, but can take identical or different values at the inner and outer walls. Our general solutions remain valid even when $Br = 0$, except for identical wall temperatures which requires a completely different approach. Note, that the combined situation with imposed heat flux at one wall and imposed wall temperature at the other wall is not addressed here.

Since the fluid properties are taken as independent of temperature, the fluid dynamic problem is decoupled from

* Corresponding author. Address: Centro de Estudos de Fenómenos de Transporte, Faculdade de Engenharia, Universidade do Porto, Rua Dr. Roberto Frias s/n, 4200-465 Porto, Portugal. Tel.: +351 225 081 762; fax: +351 225 081 763.
E-mail addresses: pmc@fe.up.pt (P.M. Coelho), fpinho@fe.up.pt (F.T. Pinho).

0017-9310/$ - see front matter © 2006 Elsevier Ltd. All rights reserved.
doi:10.1016/j.ijheatmasstransfer.2006.03.017

Nomenclature

Br	Brinkman number, Eq. (10) for wall flux BC and Eq. (27) for temperature BC
D_H	hydraulic diameter, $D_H \equiv 2\delta$
c_1, c_2, c_3, c_4	constants of integration
c_p	specific heat
h	heat transfer coefficient
k	thermal conductivity
Nu	Nusselt number, $Nu \equiv 2\delta h/k$
$p_{,x}$	axial pressure gradient
Pr	Prandtl number, $Pr = \eta c_p/k$
$\dot{q}$	heat flux
r	radial coordinate
Re	Reynolds number, $Re = \rho U 2\delta/\eta$
R_i	inner radius of concentric annulus
R_o	outer radius of concentric annulus
T	fluid temperature
$\overline{T}$	mass-averaged temperature
T^+	normalised temperature for the uniform wall heat flux case, Eq. (8a)
T'	normalised temperature for the uniform wall heat flux case, Eq. (8b)
T^*	normalised temperature for the uniform wall temperature case, Eq. (19)
u	axial velocity
u^+	normalised axial velocity, $u^+ \equiv u/U$
U	bulk velocity
U_c	characteristic velocity, $U_c = -p_{,x}\delta^2/(8\eta)$
x	axial coordinate
x'	normalised axial coordinate, $x' \equiv 2x/(\delta Re\, Pr)$
X	ratio of characteristic and bulk velocities, Eq. (6)
y^+	radius normalised by inner radius, $y^+ = r/R_i = r/(\delta Y)$
y_*^+	non-dimensional zero shear stress radius, Eq. (7)
Y	geometric parameter, $Y = \kappa/(1-\kappa)$

Greek symbols

δ	annular gap ($\delta \equiv R_o - R_i$)
Φ	ratio of outer and inner wall heat fluxes, $\Phi \equiv \dot{q}_o/\dot{q}_i$
η	dynamic viscosity of fluid
κ	radius ratio ($\kappa \equiv R_i/R_o$)
τ_{rx}	shear stress
Ω	parameter, $\Omega \equiv 4BrX$
Ψ	parameter, $\Psi \equiv 4XY^4 y_*^{+2}$

Subscripts

i	refers to inner wall
in	refers to inlet
o	refers to outer wall
w	refers to any wall

the thermal problem. The solution of the fully-developed isothermal annular flow was obtained in the XIXth century following the seminal work of Boussinesq in 1868, according to Lamb [14] and Shah and London [24].

In the absence of viscous dissipation the energy equation is homogenous and linear and the superposition principle can be used to obtain solutions for complex situations made from linear combinations of simples cases, as is explained in any basic Heat Transfer textbook (for instance, see [4]). For the so-called four fundamental types of boundary conditions in doubly connected ducts this problem has been completely solved by Lundberg et al. [16,17], according to Shah and London [24], including the corresponding thermal entry-length problems. For other boundary conditions, such as a specific variable wall temperature or heat flux, Shah and London [24] present an extensive list of works.

Available literature on heat transfer with viscous dissipation is scarcer than for the homogenous case. For fully-developed pipe and channel flows, analytical solutions have been obtained originally by Brinkman [3] and Ou and Cheng [22]. For non-Newtonian power-law fluids (thus including the Newtonian case) Toor [25] and Gill [9] presented analytical solutions for the Graetz problem and fully-developed flow in pipes, respectively. Forrest and Wilkinson [8] added temperature effects in their numerical investigation of the Graetz pipe flow problem with constant wall temperature. Recently, effects of viscous dissipation have been investigated analytically in the context of flow through porous media: Kuznetsov et al. [13] studied the Graetz problem in a fully-developed pipe flow through a porous medium for constant wall temperature, and Nield et al. [20] investigated fully-developed channel flow through a saturated medium with walls either at uniform temperature or uniform heat flux. Other heat transfer investigations for Newtonian pipe flow with viscous dissipation are listed in page 218 of Bird et al. [2].

For annular flow the available solutions are few and usually do not account for viscous dissipation. It is the case of Lundberg et al. [16,17] and Reynolds et al. [23] for Newtonian fluids and of Hong and Matthews [11] for power-law fluids, the latter case referring to the Graetz problem and listing a few other studies, all without viscous dissipation. Exceptions to this state of affairs are the analytical work of Urbanovich [26] and the numerical investigation of Lin [15]. Unfortunately, the former solution is wrong since Urbanovich ignored the effect of internal heat generation in the streamwise term of the thermal energy balance. Lin [15] also accounted for viscous dissipation in their investigation of Couette–Poiseuille flows of power-law fluids for constant wall temperature. The recent investigations of Herwig and Klemp [10] and Moghadam and Aung [19]

for Newtonian annular flow were also numerical, but neglected viscous dissipation and concentrated on assessing the effect of variable properties. The more recent extensive investigations of Manglik and Fang [18] and Fang et al. [7] for flow of Newtonian and non-Newtonian fluids in concentric and eccentric annuli are again numerical and also do not account for viscous dissipation. Neither, there is any mention of work done for concentric annuli with Newtonian fluids, and accounting for viscous dissipation, in the extensive literature survey of Fang and Manglik [6].

Therefore, as far as we are aware of, solutions are lacking for heat transfer in concentric annular flows of very viscous Newtonian fluids, including effects of viscous dissipation for at least any combination of imposed heat fluxes or imposed temperatures at both walls for which this paper presents analytical solutions.

The remaining of this paper is organized as follows: in Section 2 the thermal energy conservation equation and the fully-developed hydrodynamic solution are presented. This is followed in Sections 3 and 4 by the presentation of the solutions for imposed wall heat fluxes and imposed wall temperatures, respectively. In each of these sections the thermal energy equation is normalised first and various thermal quantities are defined prior to the presentation of the final analytical solution. To complement the analytical expressions, we present in each section some results in tabular form and discuss some results. The paper ends with a summary of the main results and conclusions.

2. Governing equations

The two cases considered are for dynamic and thermally fully-developed steady laminar flow of Newtonian fluids in concentric annuli with temperature independent properties and accounting for internal viscous heating of the fluid. The annulus has inner and outer walls of radii R_i and R_o, respectively, defining the radius ratio $\kappa \equiv R_i/R_o$ and annular gap $\delta \equiv R_o - R_i$.

The energy equation to be solved is

$$k\frac{1}{r}\frac{\partial}{\partial r}\left(r\frac{\partial T}{\partial r}\right) + \tau_{rx}\frac{\mathrm{d}u}{\mathrm{d}r} = \rho c_p u\frac{\partial T}{\partial x}, \tag{1}$$

where the temperature T varies with the axial and radial coordinates, denoted x and r, respectively, and k, ρ and c_p are the thermal conductivity, density and specific heat, respectively. The second term on the left-hand-side accounts for viscous dissipation with u representing the axial velocity and τ_{xr} the shear stress.

This second order differential equation is solved subject to two types of boundary conditions, to be imposed separately:

(1) peripherally and axially constant heat fluxes at both walls

$$r = R_i \rightarrow -k\frac{\partial T}{\partial r} = \dot{q}_i \tag{2a}$$

$$r = R_o \rightarrow T = T_o(x) \tag{2b}$$

with the outer wall heat flux imposed later when calculating the streamwise derivative of the bulk temperature;

(2) peripherally and axially constant wall temperatures

$$r = R_i \rightarrow T = T_i \tag{3a}$$

$$r = R_o \rightarrow T = T_o \tag{3b}$$

The fluid properties are taken as independent of fluid temperature, therefore the thermal problem is decoupled from the fluid dynamic solution. This fully-developed flow solution is available in the literature and is written here in non-dimensional form for the velocity in Eq. (4) and for the shear stress in Eq. (5).

$$u^+ \equiv \frac{u}{U} = 4XY^2 y_*^{+2}\left[\ln y^+ - \frac{y^{+2}-1}{2y_*^{+2}}\right] \tag{4}$$

$$\tau_{rx}^+ \equiv \frac{\tau_{rx}}{\eta U/\delta} = 4XYy_*^+\left(\frac{y_*^+}{y^+} - \frac{y^+}{y_*^+}\right) \rightarrow \tau_{rx}^+ = \frac{1}{Y}\frac{\mathrm{d}u^+}{\mathrm{d}y^+} \tag{5}$$

In these equations U represents the bulk velocity and X is the ratio between a characteristic (U_c) and the bulk velocities ($X \equiv U_c/U$). The characteristic velocity U_c is a normalisation of the constant pressure gradient, $U_c = -p_{,x}\delta^2/(8\eta)$ with η denoting the dynamic viscosity of the fluid. Y is a geometric parameter ($Y = \kappa/(1-\kappa)$), y^+ is the radius normalised by the inner cylinder radius ($y^+ = r/R_i$) and y_*^+ is the non-dimensional radius for zero shear stress. X and y_*^+ are given by Eqs. (6) and (7), respectively.

$$X = \frac{(\kappa-1)^2\ln\left(\frac{1}{\kappa}\right)}{(\kappa^2+1)\ln\left(\frac{1}{\kappa}\right) + (\kappa^2-1)} \tag{6}$$

$$y_*^+ = \sqrt{\frac{1-\kappa^2}{2\kappa^2\ln(1/\kappa)}} \tag{7}$$

Prior to its integration, the energy equation is made non-dimensional for generality, but since the normalisation is problem-dependent this is carried out separately in Section 3.

3. Solution for imposed uniform wall heat fluxes

3.1. Non-dimensional energy equation

For imposed uniform wall heat fluxes it is easy to demonstrate that $\partial T/\partial x = \partial T_w/\partial x = \partial \overline{T}/\partial x$ is a constant (c.f. [4]), with the subscript w denoting any wall and the overbar denoting mass averaging. To make the energy equation non-dimensional for this problem, two different normalisations are used for the temperature. For the terms on the left-hand-side of Eq. (1) the definition embodied in Eq. (8a) is used, based on the temperature at the outer wall ($T_o(x)$), whereas for the right-hand-side of Eq. (1) the above equality of the longitudinal temperature gradient is used together with the normalisation of Eq. (8b), where T_{in} represents the inlet temperature.

$$T^+ \equiv \frac{T - T_o}{2\delta\dot{q}/k} \tag{8a}$$

$$\overline{T}' \equiv \frac{\overline{T} - T_{in}}{2\delta\dot{q}/k} \tag{8b}$$

The axial coordinate is normalised as $x' \equiv 2x/(\delta Re\, Pr)$, with the Reynolds and Prandtl numbers defined as $Re = \rho U 2\delta/\eta$ and $Pr = \eta c_p/k$, and Eq. (1) becomes

$$\frac{1}{y^+}\frac{\partial}{\partial y^+}\left(y^+\frac{\partial T^+}{\partial y^+}\right) + YBr\tau_{rx}^+\frac{\mathrm{d}u^+}{\mathrm{d}y^+} = Y^2u^+\frac{\mathrm{d}\overline{T}'}{\mathrm{d}x'} \tag{9}$$

where the derivative on the right-hand-side is a constant, discussed below and the Brinkman number Br is defined in Eq. (10).

$$Br = \frac{\eta U^2}{2\delta\dot{q}} \tag{10}$$

This definition is adequate for general problems with imposed wall heat flux since the fluxes can be arbitrarily defined. However, the use of the perimeter-average wall heat flux $\dot{q}$ of Eq. (11), based on the inner ($\dot{q}_\mathrm{i}$) and outer ($\dot{q}_\mathrm{o}$) wall heat fluxes, turns Br into a quantity dependent on κ. This definition is not usual in the less general solutions found in the literature and must be taken into account when performing comparisons. The perimeter-average wall heat flux is

$$\dot{q} = \frac{\dot{q}_\mathrm{i}R_\mathrm{i} + \dot{q}_\mathrm{o}R_\mathrm{o}}{R_\mathrm{i}+R_\mathrm{o}} = \dot{q}_\mathrm{i}\frac{\kappa+\Phi}{1+\kappa} \tag{11}$$

where Φ stands for the ratio between the outer and inner wall heat fluxes, $\Phi \equiv \dot{q}_\mathrm{o}/\dot{q}_\mathrm{i}$.

The non-dimensional heat flux boundary conditions (Eqs. (2a) and (2b)) take the forms

$$y^+ = y_\mathrm{i}^+ = 1 \rightarrow \frac{\partial T^+}{\partial y^+} = \frac{\kappa(\kappa+1)}{2(\kappa+\Phi)(\kappa-1)} \tag{12a}$$

$$y^+ = y_\mathrm{o}^+ = \frac{1}{\kappa} \rightarrow T^+ = 0 \tag{12b}$$

The outer wall boundary condition is a consequence of the normalisation used for temperature, c.f. Eq. (8a). The outer wall heat flux is indirectly imposed when the derivative on the right-hand-side of Eq. (9) is calculated with the following energy balance over a control volume encompassing the annulus and both walls.

$$\begin{aligned}&\dot{q}_\mathrm{i}2\pi R_\mathrm{i}\mathrm{d}x + \dot{q}_\mathrm{o}2\pi R_\mathrm{o}\mathrm{d}x + U2\pi(R_\mathrm{i}|\tau_\mathrm{wi}| + R_\mathrm{o}|\tau_\mathrm{wo}|)\mathrm{d}x\\ &\quad = \rho U\pi(R_\mathrm{o}^2 - R_\mathrm{i}^2)c_p\mathrm{d}\overline{T}\end{aligned} \tag{13}$$

leading to the following constant streamwise gradient of non-dimensional bulk temperature:

$$\frac{\mathrm{d}\overline{T}'}{\mathrm{d}x'} = 1 + 8BrX \tag{14}$$

Hence, the non-dimensional energy equation contains a single definition of non-dimensional temperature. Note that when presenting the final solution for the bulk temperature in Section 3.2, the definition $\overline{T}^+$ appears naturally.

3.2. Analytical solution

Integration of the energy equation (Eq. (9)) was carried out with the help of the symbolic mathematics code Derive 5 from Texas Instruments.

The heat transfer from the walls to the fluid was quantified via the inner wall (Nu_i) and outer wall (Nu_o) Nusselt numbers. Each Nusselt number is defined as $Nu \equiv 2\delta h/k$, where the hydraulic diameter ($D_\mathrm{H} \equiv 2\delta$) is used, and h is the heat transfer coefficient at that wall calculated from $\dot{q}_\mathrm{w} = h_\mathrm{w}(T_\mathrm{w} - \overline{T})$. Normalising temperatures by Eq. (8a), the Nusselt number becomes $Nu_\mathrm{w} = \dot{q}_\mathrm{w}/[\dot{q}(T_\mathrm{w}^+ - \overline{T}^+)]$ and using Eq. (11) leads to expressions based on temperature:

– at the inner wall,

$$Nu_\mathrm{i} = \frac{(1+\kappa)}{(\kappa+\Phi)}\frac{1}{(T_\mathrm{i}^+ - \overline{T}^+)} \tag{15a}$$

– at the outer wall,

$$Nu_\mathrm{o} = \frac{\Phi(1+\kappa)}{(\kappa+\Phi)}\frac{1}{(T_\mathrm{o}^+ - \overline{T}^+)} \tag{15b}$$

The wall temperatures were calculated from the derived temperature profile and the normalised bulk temperature was calculated with the following integration:

$$\overline{T}^+ = \int_1^{1/\kappa} 2\frac{\kappa^2}{1-\kappa^2}u^+T^+y^+\mathrm{d}y^+ \tag{16}$$

The analytical solution is given by long equations presented in Appendix, Part 1, at the end. Here, the simple equation for the temperature profile is presented together with compact expressions for the Nusselt numbers useful for engineering calculations.

The non-dimensional temperature profile, $T^+(y^+)$ is given by

$$\begin{aligned}T^+ = &-\frac{\Omega\Psi y_*^{+2}(\ln y^+)^2}{2} + \left[\frac{\Psi y^{+2}(2\Omega+1)}{4} + \Psi c_1\right]\ln y^+\\ &-\frac{\Psi[y^{+4}(4\Omega+1) - 4y^{+2}(2\Omega - 2y_*^{+2}+1) - 32y_*^{+2}c_2]}{32y_*^{+2}}\end{aligned} \tag{17}$$

where parameters $\Omega = 4BrX$ and $\Psi = 4Xy_*^{+2}Y^4$ and the integration constants c_1 and c_2 are

$$c_1 = \frac{\Psi(\kappa+\Phi)(\kappa-1)(4\Omega y_*^{+2} - 2y_*^{+2}+1) - 4\kappa y_*^{+2}(\kappa+1)}{8\Psi y_*^{+2}(1-\kappa)(\kappa+\Phi)} \tag{18}$$

$$\begin{aligned}c_2 = &\frac{\Omega y_*^{+2}(\ln\kappa)^2}{2} - \frac{4\Omega(2\kappa^2-1) + 4\kappa^2(1-2y_*^{+2}) - 1}{32\kappa^4 y_*^{+2}}\\ &+\frac{\{\Psi(\kappa+\Phi)(\kappa-1)[4\Omega y_*^{+2}(\kappa^2-1) + \kappa^2(1-2y_*^{+2}) - 2y_*^{+2}] - 4\kappa^3 y_*^{+2}(\kappa+1)\}\ln\kappa}{8\Psi\kappa^2 y_*^{+2}(1-\kappa)(\kappa+\Phi)}\end{aligned} \tag{19}$$

Compact expressions are useful for engineering calculations and the following equations for the inner and outer walls Nusselt numbers were produced from the exact expressions in Appendix A.

$$Nu_i = \frac{\alpha_1}{Br\left(\frac{\Phi}{\kappa}+1\right)+\alpha_2\cdot\Phi+\alpha_3} \tag{20a}$$

$$Nu_o = \frac{\alpha_1\cdot\Phi}{Br\left(\frac{\Phi}{\kappa}+1\right)+\beta_1\cdot\Phi+\beta_2} \tag{20b}$$

Coefficients α_i and β_i depend on the radius ratio κ taking the values listed in Table 1. These coefficients are exact to within five significant digits since they were calculated from the analytical equations in Appendix A for the specific values of the radius ratio κ in Table 1 and so the equations provide the same degree of accuracy for the Nusselt number regardless of Br and Φ, i.e., exact values in practical terms. However, for different values of κ the accuracy in Nu of Eq. (20) depends on the interpolation method used to determine the coefficients α and β. As an example, use of linear interpolation to determine the coefficients for $\kappa = 0.45$ leads to values of Nu_i and Nu_o accurate within 1%. Better accuracy requires the use of higher order interpolation schemes.

The analytical solution has limiting cases, some of which have been obtained previously, and were used here to check the validity of our solution: (i) the channel flow with identical wall heat fluxes and viscous dissipation of Oliveira and Pinho [21] and Nield et al. [20] (in this latter work it is necessary to consider zero porosity of the porous media inside the channel); (ii) the pipe flow with viscous dissipation of Oliveira and Pinho [21], (iii) the channel flow without viscous dissipation of Shah and London [24] (their Eq. 273). In all these cases our solutions match exactly the analytical and numerical data in the literature.

A particularly interesting annular flow case corresponds to heating or cooling at both walls leading to identical wall temperatures ($T_i^+ = T_o^+$). This happens for a heat flux ratio of

$$\Phi_c = -\frac{\kappa[4(\ln\kappa)^2+(1-\kappa^2)(3\kappa^2+7)\ln\kappa+4(\kappa^2-1)^2]}{4\kappa^4(\ln\kappa)^2+(1-\kappa^2)(7\kappa^2+3)\ln\kappa+4(\kappa^2-1)^2} \tag{21}$$

Table 1
Coefficients for the Nusselt number equations (20a) and (20b)

κ	α_1	α_2	α_3	β_1	β_2
0.02	59.211	−7.5757	1.8104	12.507	−0.15151
0.05	25.078	−3.0737	1.4080	5.2333	−0.15369
0.1	13.463	−1.5645	1.1308	2.7849	−0.15645
0.2	7.5287	−0.80097	0.88584	1.5419	−0.16019
0.3	5.5087	−0.54185	0.76075	1.1178	−0.16256
0.4	4.4840	−0.41026	0.68112	0.90055	−0.16411
0.5	3.8622	−0.33027	0.62485	0.76683	−0.16513
0.6	3.4437	−0.27635	0.58252	0.67534	−0.16581
0.7	3.1423	−0.23749	0.54931	0.60824	−0.16624
0.8	2.9145	−0.20812	0.52246	0.55657	−0.16650
0.9	2.7362	−0.18514	0.50021	0.51533	−0.16663
1	2.5926	−0.16667	0.48148	0.48148	−0.16667

which is independent of the Brinkman number. However, the amount of viscous dissipation affects the bulk temperature and the corresponding Nusselt numbers are

$$Nu_o = \frac{72(1-\kappa)[4(\ln\kappa)^2+(1-\kappa^2)(3\kappa^2+7)\ln\kappa+4(\kappa^2-1)^2][(1+\kappa^2)\ln\kappa+1-\kappa^2]^2}{A(\ln\kappa)^4+B(\ln\kappa)^3+C(\ln\kappa)^2+D(\ln\kappa)+144(\kappa^2-1)^4} \tag{22}$$

$$Nu_i = \frac{Nu_o}{\Phi_c} \tag{23}$$

with coefficients A, B, C and D of

$$A = 6(\kappa^6+\kappa^4+\kappa^2+1)[48Br(\kappa-1)^2+11(\kappa^2+1)]$$

$$B = [1056Br(\kappa^6-2\kappa^5+2\kappa^4-2\kappa^3+2\kappa^2-2\kappa+1)+299\kappa^6+613\kappa^4+613\kappa^2+299](1-\kappa^2)$$

$$C = (\kappa^2-1)^2[1512Br(\kappa^4-2\kappa^3+2\kappa^2-2\kappa+1)+539\kappa^4+926\kappa^2+539]$$

$$D = 18(1-\kappa^2)^3[48Br(\kappa-1)^2+25(\kappa^2+1)]$$

3.3. Discussion of results

Here, we analyze some results for imposed uniform wall heat fluxes. These are positive when heating the fluid, whereas a negative sign implies cooling.

For simultaneous wall heating or cooling at both walls the heat flux ratio is positive, whereas the Brinkman number, Eq. (10), is positive for the former and negative for the latter cases.

In general, viscous dissipation reduces the Nusselt numbers, because viscous heating increases the fluid temperature range within the annulus leading to higher differences between the wall and bulk temperatures. This difference appears in the denominator of the convective heat transfer coefficients. Exceptions to this behaviour occur whenever there is a change in the sign of this temperature difference leading to singularities in the Nusselt numbers. These are seen in Figs. 1 and 2, for the inner and outer Nusselt numbers, respectively, in an annulus of $\kappa = 0.5$ and for intermediate values of Φ. For $\Phi \leqslant 0.01$ the heat transfer characteristics are basically independent of Φ and correspond to those of an annulus with insulated outer wall. Correspondingly, for $\Phi \geqslant 100$ the flow behaves as in annulus with insulated inner wall.

In both figures, the Nusselt number approaches infinity when the bulk temperature approaches the wall temperature, followed by a change of sign corresponding to a change in their relative magnitudes. This is due first to the heating/cooling effect of the other wall, but especially because of the strong influence of the extra heat generated by viscous dissipation interfering with the relative magnitudes of bulk and wall temperatures. The change in the relative magnitudes of the wall and bulk temperatures is well shown in the temperature profiles of Fig. 3, which emphasizes the role of viscous dissipation. Only for small values of Br (regardless of whether there is wall heating or cooling) are the fluid and bulk temperatures limited by the two wall temperatures.

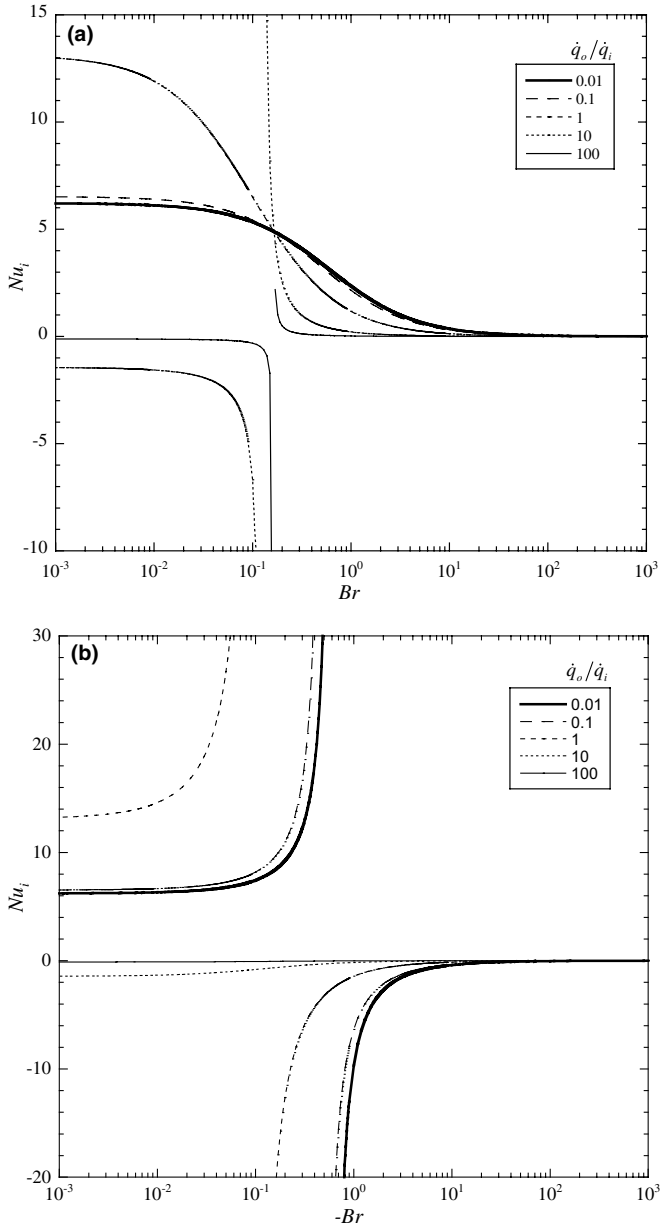

Fig. 1. Variation of the inner wall Nusselt number with the heat flux ratio and Brinkman number for a radius ratio of 0.5: (a) $Br > 0$; (b) $Br < 0$.

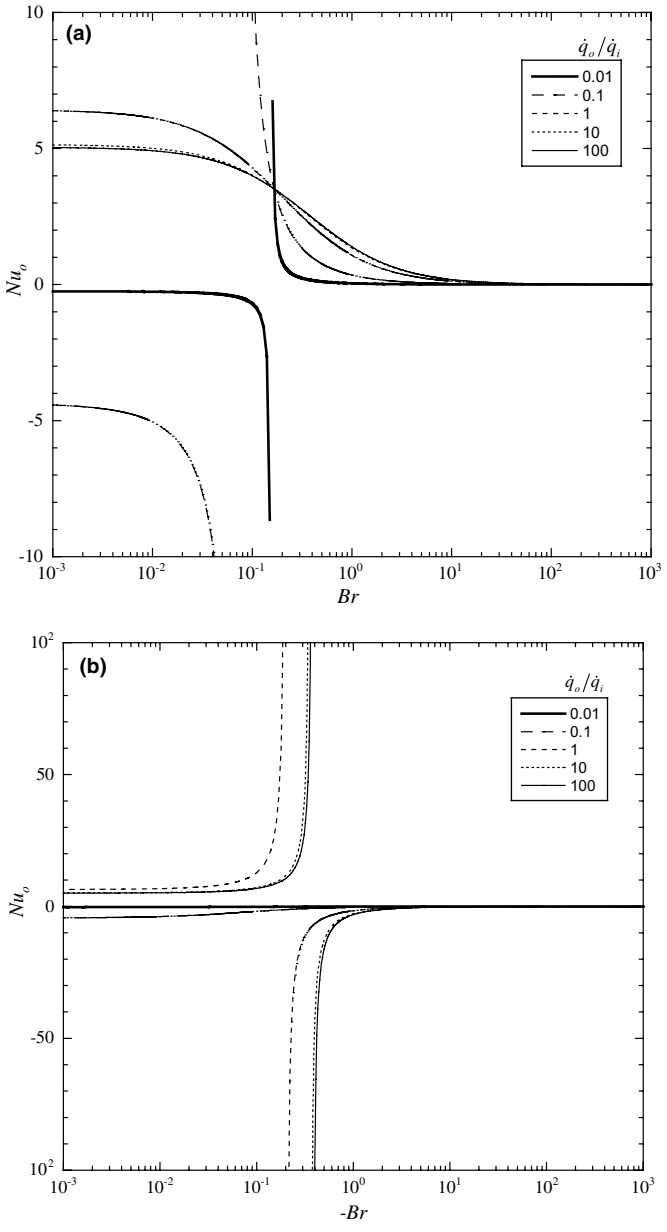

Fig. 2. Variation of the outer wall Nusselt number with the heat flux ratio and Brinkman number for a radius ratio of 0.5: (a) $Br > 0$; (b) $Br < 0$.

4. Solution for imposed uniform temperatures at walls

4.1. Non-dimensional energy equation

For this problem two normalisations are also used for temperature and we must distinguish between different and identical wall temperatures. The non-dimensional temperature appearing in the energy equation T^* is defined in Eq. (24).

$$T^* = \frac{T - T_\mathrm{i}}{T_\mathrm{o} - T_\mathrm{i}} \quad \text{when } T_\mathrm{i} \neq T_\mathrm{o} \tag{24a}$$

$$T^* = \frac{T - T_\mathrm{in}}{T_\mathrm{w} - T_\mathrm{in}} \quad \text{when } T_\mathrm{w} = T_\mathrm{i} = T_\mathrm{o} \tag{24b}$$

Only the asymptotic solution, for which $\partial\overline{T}/\partial x = 0$, will be presented here, since the asymptotic solution without viscous dissipation for $T_\mathrm{i} = T_\mathrm{o}$ has already been obtained (see [24]). Upon substitution of the shear rate and shear stress expressions, the non-dimensional energy Eq. (2) becomes

$$\frac{1}{y^+}\frac{\partial}{\partial y^+}\left(y^+\frac{\partial T^*}{\partial y^+}\right) + Br\left[4XY^2 y_*^+\left(\frac{y_*^+}{y^+} - \frac{y^+}{y_*^+}\right)\right]^2 = 0 \tag{25}$$

The boundary conditions and the Brinkman number are defined differently for different and identical wall temperatures, as follows:

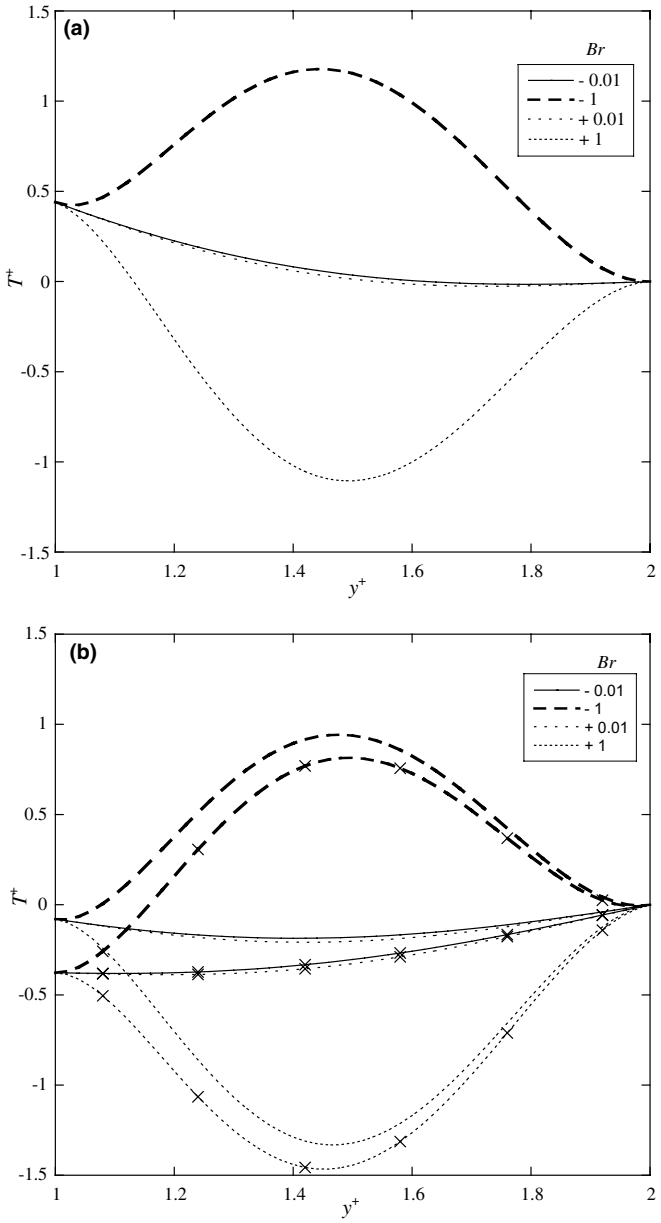

Fig. 3. Temperature variation across a $\kappa = 0.5$ annulus as a function of the Brinkman number: (a) $\dot{q}_0/\dot{q}_i = 0.1$; (b) $\dot{q}_0/\dot{q}_i = 1$ (no symbols), $\dot{q}_0/\dot{q}_i = 10$ (with symbols).

(1) $T_o \neq T_i$

$$\text{inner wall}: \; y^+ = 1 \rightarrow T_i^* = 0; \qquad \text{outer wall}: \; y^+ = \frac{1}{\kappa} \rightarrow T_o^* = 1 \tag{26}$$

$$Br = \frac{\eta U^2}{k(T_o - T_i)} \tag{27}$$

Setting $Br = 0$ we recover the solution of Shah and London [24] as it should be whereas for $Br \rightarrow \infty$ we get the same solution as for identical wall temperatures and for which both Nu values are independent of Br.

(2) $T_w = T_o = T_i$,

$$Br = \frac{\eta U^2}{k(T_w - T_{in})} \tag{28}$$

$$\text{inner wall}: \; y^+ = 1 \rightarrow T_i^* = 1; \qquad \text{outer wall}: \; y^+ = \frac{1}{\kappa} \rightarrow T_o^* = 1 \tag{29}$$

4.2. Analytical solution

The Nusselt numbers at the inner and outer walls are defined in Eqs. (30a) and (30b), respectively.

$$Nu_i = -\frac{2}{Y}\frac{\left.\frac{dT^*}{dy^+}\right|_{y^+=1}}{T_i^* - \overline{T}^*} \tag{30a}$$

$$Nu_o = \frac{2}{Y}\frac{\left.\frac{dT^*}{dy^+}\right|_{y^+=\frac{1}{\kappa}}}{T_o^* - \overline{T}^*} \tag{30b}$$

The bulk temperature is calculated as in Eq. (16), except for the use of the different non-dimensional temperature. Therefore, it is now given by

$$\overline{T}^* = \int_1^{1/\kappa} 2\frac{\kappa^2}{1-\kappa^2} u^+ T^* y^+ dy^+ \tag{31}$$

The analytical solution for different and identical wall temperatures are the same, except for the different definitions above of the Brinkman number, normalised temperature and inner wall temperature. As a consequence the constants of integration c_3 and c_4 also differ. Below, only the simple expression for the temperature profile is presented together with compact expressions for the Nusselt numbers, useful for engineering calculations. The equations for the other quantities are presented in Appendix, Part 2.

The non-dimensional temperature profile, T^* is

$$T^* = -\frac{\Psi\Omega y_*^{+^2}(\ln y^+)^2}{2} + \Psi\Omega c_3 \ln y^+ - \frac{\Psi\Omega(y^{+^4} - 8y_*^{+^2}y^{+^2} - 16c_4 y_*^{+^2})}{16y_*^{+^2}} \tag{32}$$

with integration constants c_3 and c_4 depending on the boundary conditions. For different wall temperatures ($T_i \neq T_o$)

$$c_3 = -\frac{y_*^{+^2}\ln\kappa}{2} - \frac{\Psi\Omega[\kappa^4(8y_*^{+^2} - 1) - 8\kappa^2 y_*^{+^2} + 1] + 16\kappa^4 y_*^{+^2}}{16\Psi\Omega\kappa^4 y_*^{+^2}\ln\kappa} \tag{33}$$

$$c_4 = \frac{1 - 8y_*^{+^2}}{16y_*^{+^2}} \tag{34}$$

whereas for identical wall temperatures ($T_i = T_o$)

$$c_3 = -\frac{y_*^{+^2}\ln\kappa}{2} - \frac{\kappa^4(8y_*^{+^2} - 1) - 8\kappa^2 y_*^{+^2} + 1}{16\kappa^4 y_*^{+^2}\ln\kappa} \tag{35}$$

$$c_4 = \frac{1}{\Psi\Omega} + \frac{1 - 8y_*^{+^2}}{16y_*^{+^2}} \tag{36}$$

The exact solution was compared with limiting cases of pipe and channel flow and the result match those in Coelho

Table 2
Coefficients for the Nusselt number equations (37) and (38)

κ	χ_1	χ_2	χ_3	ε_1	ε_2	ε_2
0	–	–	–	9.6	0	0
0.02	118.46	33.198	1.1002	11.573	−0.66396	−0.22520
0.05	64.509	17.199	1.0710	12.127	−0.85996	−0.28486
0.1	42.970	10.823	1.0349	12.717	−1.0823	−0.34967
0.2	30.329	7.0353	0.97749	13.541	−1.4071	−0.43788
0.3	25.506	5.5513	0.93044	14.189	−1.6654	−0.50176
0.4	22.883	4.7227	0.89022	14.755	−1.8891	−0.55224
0.5	21.210	4.1809	0.85517	15.273	−2.0904	−0.59382
0.6	20.039	3.7930	0.82423	15.757	−2.2758	−0.62893
0.7	19.168	3.4985	0.79667	16.218	−2.4489	−0.65912
0.8	18.491	3.2655	0.77191	16.659	−2.6124	−0.68542
0.9	17.947	3.0754	0.74953	17.086	−2.7678	−0.70858
1	17.5	2.9167	0.72917	17.5	−2.9167	−0.72917

et al. [5] for imposed constant wall temperature for Newtonian fluids.

For ease of use, Eqs. (37) and (38) present simple expressions for the Nusselt numbers at the inner and outer walls respectively, as a function of the Brinkman number for the case of different wall temperatures. Their coefficients depend on κ as listed in Table 2 and are exact to within five significant digits since they were calculated from the analytical equations in Appendix A for those specific values of the radius ratio κ listed, i.e., these equations provide the same degree of accuracy for the Nusselt number regardless of Br, which in practical term means exact values. However, for values of κ not in Table 2 the accuracy in Nu as given by Eqs. (37) and (38) depends on the interpolation methods used to determine the coefficients χ and ε. As an example, the use of linear interpolation to determine the coefficients for $\kappa = 0.45$ leads to values of Nu_i and Nu_o accurate within 1%. Better accuracy requires the use of higher order interpolation schemes.

$$Nu_i = \frac{\chi_1 \cdot Br + \chi_2}{Br + \chi_3} \tag{37}$$

$$Nu_o = \frac{\varepsilon_1 \cdot Br + \varepsilon_2}{Br + \varepsilon_3} \tag{38}$$

When the wall temperatures are identical, $Nu_i = \chi_1$ and $Nu_o = \varepsilon_1$, i.e., there is no effect of the Brinkman number.

4.3. Discussion of results

Some of the results for different wall temperatures ($T_i \neq T_o$) are discussed with the help of Figs. 4 and 5. Now, a positive Brinkman number, Eq. (27), means that the outer wall temperature is higher than the inner wall temperature and vice versa for a negative Brinkman number. Two other conditions are to be considered: for low values of $|Br|$ fluid heats at the warmer wall and cools at the colder wall whereas for large values of $|Br|$ the internal heat generation raises the fluid temperature above the higher wall temperature and the fluid cools at both walls. The critical Brinkman number separating these two thermal conditions corresponds to the warmer wall behaving as an

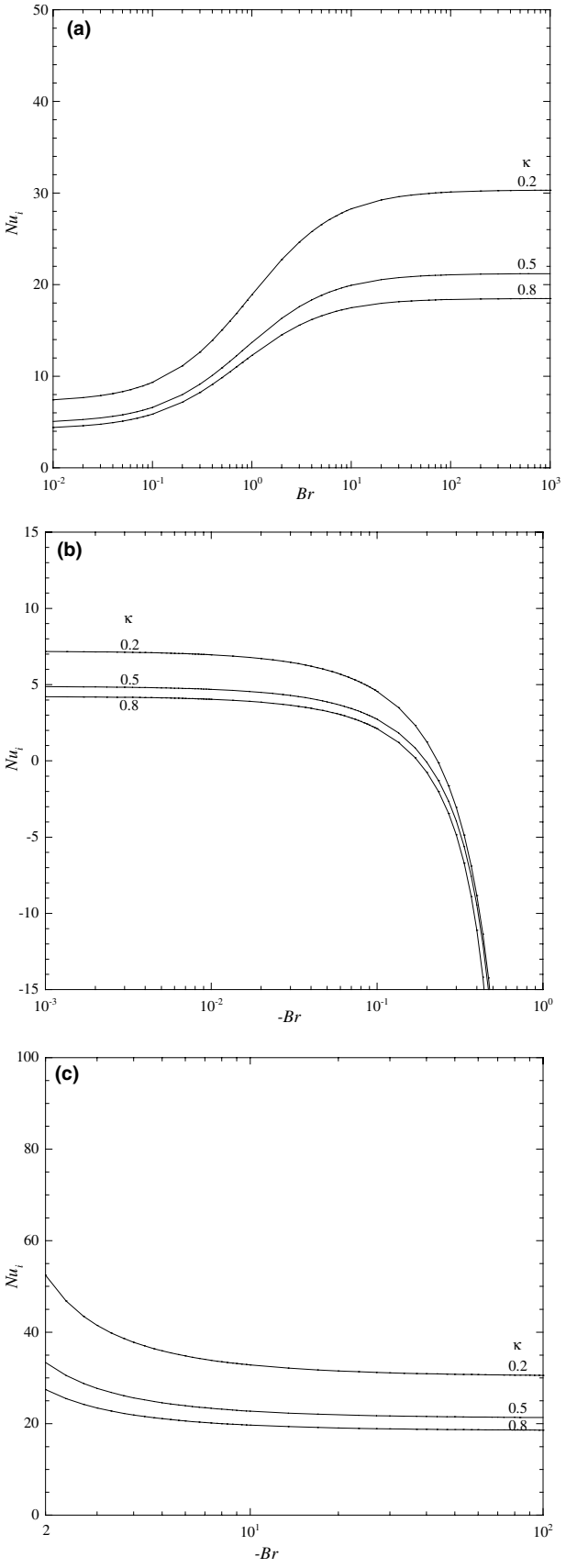

Fig. 4. Variation of the inner wall Nusselt number with the Brinkman number and radius ratio: (a) $Br > 0$; (b) $-1 \leqslant Br \leqslant 0$; (c) $-100 \leqslant Br \leqslant -2$.

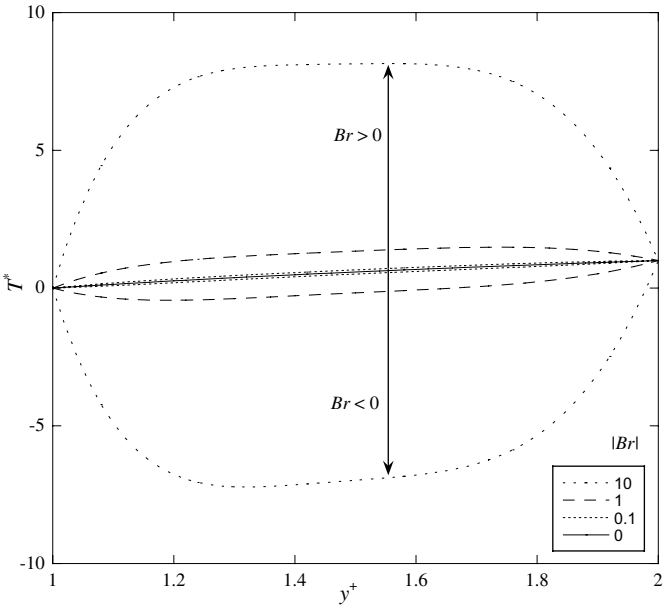

Fig. 5. Temperature profile T^* across the annulus as a function of the Brinkman number for $\kappa = 0.5$.

insulated wall, i.e., $dT^*/dy^+|_{wall} = 0$ and is given by Eq. (39a) for $T_i^* > T_o^*$ and Eq. (39b) for $T_i^* < T_o^*$

$$Br_c = -\frac{[(1+\kappa^2)\ln\kappa + 1 - \kappa^2]^2}{\ln\kappa[4\kappa^4(\ln\kappa)^2 + (1-\kappa^2)(7\kappa^2+3)\ln\kappa + 4(\kappa^2-1)^2]} \tag{39a}$$

$$Br_c = -\frac{[(1+\kappa^2)\ln\kappa + 1 - \kappa^2]^2}{\ln\kappa[4(\ln\kappa)^2 + (1-\kappa^2)(3\kappa^2+7)\ln\kappa + 4(\kappa^2-1)^2]} \tag{39b}$$

Both these critical Brinkman numbers increase as κ increases from 0 to 1, exhibiting a steep gradient near $\kappa = 0$: for $T_i^* > T_o^*$, Br_c increases from -0.33 to -0.167, whereas for $T_i^* < T_o^*$ it increases from 0 to $+0.167$. For each value of the radius ratio the Nusselt numbers show singularities at both Br_c.

In Fig. 4, the variation of the inner Nusselt number with the Brinkman number and the radius ratio is plotted. For $Br > 0$ ($T_o^* > T_i^*$), the variation of Nu_i in Fig. 4(a) is monotonic with both Br and κ, with Nu_i increasing with the former and decreasing with the latter. T_i^* is always lower than the bulk temperature $\overline{T}^*$ and the heat flux at the inner wall is always negative. When the relative magnitudes of the inner and outer wall temperatures are reversed ($T_i^* > T_o^*$), the variations of Nu_i with Br are no longer monotonic, because of the changes in the signs of the heat flux and of the temperature difference $T_i^* - \overline{T}^*$ (cf. Eq. (30)). For $dT^*/dy^+ = 0$ at the inner wall and a change of sign in the wall heat flux, the Nusselt number changes sign monotonically, as can be seen in Fig. 4(b) at $-Br \approx 0.2$–0.3, even though $T_i^* > \overline{T}^*$. However, when the bulk temperature increases due to viscous heating and $T_i^* = \overline{T}^*$, Nu_i goes through a singularity. For negative Brinkman numbers, and $\overline{T}^* > T_i^*$, the Nusselt number becomes positive again, now decreasing with viscous dissipation (Fig. 4(c)) because the temperature difference $\overline{T}^* - T_i^*$ raises faster than dT^*/dy^+ at the wall, c.f. Eq. (30).

For the outer wall Nusselt number the behaviour is of the same type as for Nu_i, although somewhat reversed, therefore no data are plotted for Nu_o.

Finally, in Fig. 5 radial profiles of normalised temperature T^* are plotted as a function of the Brinkman number for a radius ratio $\kappa = 0.5$. Profiles are shown for both positive (upper part) and negative (lower part) Brinkman numbers. For $Br > 0$, the inner wall temperature is lower than the fluid temperature, and there is increased cooling at this wall as viscous dissipation is enhanced. At the outer wall, however, in the absence of viscous dissipation (or for low Brinkman numbers) its temperature is higher than the fluid bulk temperature and consequently there is fluid heating. As internal heat generation increases the outer wall heat flux changes direction from fluid heating to fluid cooling, although initially the outer wall temperature remains higher than the bulk temperature. With further increases in viscous dissipation the bulk temperature rises above the outer wall temperature.

5. Conclusions

Analytical solutions are presented for fully-developed laminar convective heat transfer in concentric annuli of Newtonian fluids of very high viscosity (viscous dissipation included) for the following boundary conditions:

(i) imposed uniform, but different, wall heat fluxes;
(ii) imposed uniform, but different, wall temperatures.

The results are presented as explicit equations for the temperature profile, the inner and outer wall temperatures, the mixing temperature and the inner and outer Nusselt numbers, as a function of the Brinkman number, radius ratio and, for the case with imposed wall fluxes, the wall heat flux ratio. The special case of determining the wall heat flux ratio for identical wall temperatures is also analysed and for imposed wall temperatures, a solution is also given for the special case of identical wall temperatures, which can not be used for $Br = 0$.

For ease of use, compact expressions are presented of the Nusselt number as a function of the Brinkman number, with the corresponding coefficients listed in tables for specific values of the radius ratio. The exact expressions are also available in a useful manner, as FORTRAN codes at the following site http://www.fe.up.pt/~fpinho/research/menur.html.

Acknowledgement

FTP acknowledges funding by FEDER and Fundação para a Ciência e a Tecnologia through grants POCI 56342/EQU/2004 and POCI 59338/EME/2004.

Appendix A

A.1. Part 1. Analytical solution for imposed wall heat flux

The following expressions complete the analytical solution of Section 3.

– Inner wall temperature, T_{i}^{+}

$$T_{\mathrm{i}}^{+} = \frac{\Psi(4\Omega - 8y_{*}^{+2} + 3)}{32y_{*}^{+2}} + \Psi c_2 = \frac{\Psi\kappa^2(4\Omega+3)\ln\kappa}{16(\kappa^2-1)} + \frac{\Psi(4c_2-1)}{4} \tag{A.1.1}$$

– Outer wall temperature,

$$T_{\mathrm{o}}^{+} = 0 \tag{A.1.2}$$

– Bulk temperature, $\overline{T}^{+}$

$$\overline{T}^{+} = \frac{\Psi^2[3P_1(\ln\kappa)^3 + 2(1-\kappa^2)P_2(\ln\kappa)^2 - 9(\kappa^2-1)^2P_3\ln\kappa + 108\Omega(\kappa^2-1)^3]}{576Y^2\kappa^2(\kappa^2-1)^2\ln\kappa} \tag{A.1.3}$$

with

$$P_1 = (\kappa^6+\kappa^4)(12\Omega+7) + \kappa^2(36\Omega+96c_1+7) - 12\Omega + 7$$
$$P_2 = \kappa^4(24\Omega+108c_1-144c_2+25) + \kappa^2(60\Omega+252c_1-144c_2+25) - 66\Omega + 25$$
$$P_3 = \kappa^2(5\Omega-32c_1+32c_2-3) + 3(7\Omega-1)$$

– Inner wall Nusselt number, Nu_{i}

$$Nu_{\mathrm{i}} = \frac{-576\kappa^2(\kappa-1)^2(\kappa+1)^3\ln\kappa}{\Psi(\kappa+\Phi)\left[3\frac{\Psi}{Y^2}P_1(\ln\kappa)^3 + 2(1-\kappa^2)Q_1(\ln\kappa)^2 - 9(\kappa^2-1)^2Q_2\ln\kappa + 108\Omega\frac{\Psi}{Y^2}(\kappa^2-1)^3\right]} \tag{A.1.4}$$

with

$$Q_1 = \kappa^4(72\Omega+54) + \frac{\Psi}{Y^2}P_2$$
$$Q_2 = 16(4c_2-1)\kappa^2 + \frac{\Psi}{Y^2}P_3$$

– Outer wall Nusselt number, Nu_{o}

$$Nu_{\mathrm{o}} = \frac{-576\Phi\kappa^2(\kappa-1)^2(\kappa+1)^3\ln\kappa}{\frac{\Psi^2}{Y^2}(\kappa+\Phi)[3P_1(\ln\kappa)^3 + 2(1-\kappa^2)P_2(\ln\kappa)^2 - 9(\kappa^2-1)^2P_3\ln\kappa + 108\Omega(\kappa^2-1)^3]} \tag{A.1.5}$$

A.2. Part 2. Analytical solution for imposed wall temperature

The following expressions complete the analytical solution of Section 4 and are valid regardless of whether wall temperatures are equal or not, except for the constants of integration, the definitions of the Brinkman number, normalised temperature and inner wall temperature T_{i}^{*}.

– Bulk temperature, $\overline{T}^{*}$

$$\overline{T}^{*} = \frac{\Psi^2\Omega[6I_1(\ln\kappa)^3 + 4(\kappa^2-1)I_2(\ln\kappa)^2 + 9(\kappa^2-1)^2I_3\ln\kappa - 108(\kappa^2-1)^3]}{576Y^2\kappa^2(\kappa^2-1)^2\ln\kappa} \tag{A.2.1}$$

with

$$I_1 = \kappa^6 + \kappa^4 - \kappa^2(48c_3+11) + 13$$
$$I_2 = \kappa^4(54c_3-72c_4-13) + \kappa^2(126c_3-72c_4+5) - 58$$
$$I_3 = 27 - \kappa^2(32c_3-32c_4-11)$$

– Inner wall Nusselt number, Nu_{i}

$$Nu_{\mathrm{i}} = \frac{576Y^2\kappa(\kappa+1)(\kappa-1)^2\ln\kappa[2(c_3+1)(\kappa^2-1) - \kappa^2\ln\kappa]}{\Psi\Omega\{6I_1(\ln\kappa)^3 + 4(\kappa^2-1)I_2(\ln\kappa)^2 + 9(\kappa^2-1)^2[I_3 + 64\kappa^2Y^2T_{\mathrm{i}}^{*}/(\Psi^2\Omega)]\ln\kappa + 108(\kappa^2-1)^3\}} \tag{A.2.2}$$

– Outer wall Nusselt number, Nu_{o}

$$Nu_{\mathrm{o}} = \frac{576Y^2(\kappa+1)(\kappa-1)^2\ln\kappa[\ln\kappa - \kappa^4(2c_3+1) + 2c_3\kappa^2 + 1]}{\Psi\Omega\{6I_1(\ln\kappa)^3 + 4(\kappa^2-1)I_2(\ln\kappa)^2 + 9(\kappa^2-1)^2[I_3 + 64\kappa^2Y^2/(\Psi^2\Omega)]\ln\kappa - 108(\kappa^2-1)^3\}} \tag{A.2.3}$$

References

[1] J.-F. Agassant, P. Avenas, J.-Ph. Sergent, P.J. Carreau, Polymer Processing, Principles and Modeling, Hanser Publishers, Munich, 1991.

[2] R.B. Bird, R.C. Armstrong, O. Hassager, Dynamics of Polymeric Liquids. Volume 1: Fluid Mechanics, 2nd ed., John Wiley & Sons, London, 1987.

[3] H.C. Brinkman, Heat effects in capillary flow I, Appl. Sci. Res. A 2 (1951) 120–124.
[4] Y.A. Çengel, Heat Transfer, a Practical Approach, 2nd ed., McGraw-Hill, New York, 2003.
[5] P.M. Coelho, F.T. Pinho, P.J. Oliveira, Fully developed forced convection of the Phan-Thien–Tanner fluid in ducts with a constant wall temperature, Int. J. Heat Mass Transfer 45 (2002) 1413–1423.
[6] P. Fang, R.M. Manglik. Numerical investigation of laminar forced convection in Newtonian and non-Newtonian flows in eccentric annuli, Technical Report TFTPL-3, Dept. Mechanical, industrial and Nuclear Engineering, University of Cincinnati, USA, 1998.
[7] P. Fang, R.M. Manglik, M.A. Jog, Characteristics of laminar viscous shear-thinning fluid flows in eccentric annular channels, J. Non-Newt. Fluid Mech. 84 (1999) 1–17.
[8] G. Forrest, W.L. Wilkinson, Laminar heat transfer to power law fluids in tubes with constant wall temperature, Trans. Inst. Chem. Engrs. 51 (1973) 331–338.
[9] W.N. Gill, Heat transfer in laminar power law flows with energy sources, AIChEJ 8 (1) (1962) 137–138.
[10] H. Herwig, K. Klemp, Variable property effects of fully developed laminar flow in concentric annuli, J. Heat Transfer 110 (1988) 314–320.
[11] S.-N. Hong, J.C. Matthews, Heat transfer to non-Newtonian fluids in laminar flow through concentric annuli, Int. J. Heat Mass Transfer 12 (1969) 1699–1703.
[12] W.M. Kays, M.E. Crawford, B. Weigand, Convective Heat and Mass Transfer, 4th ed., McGraw-Hill, New York, 2004.
[13] A.V. Kuznetsov, M. Xiong, D.A. Nield, Thermally developing forced convection in a porous medium: circular duct with walls at constant temperature, with longitudinal conduction and viscous dissipation effects, Transport Porous Media 53 (2003) 331–345.
[14] H. Lamb, Hydrodynamics, 6th ed., Cambridge University Press, Cambridge, UK, 1932.
[15] S.H. Lin, Heat transfer to generalized non-Newtonian Couette flow in annuli with moving outer cylinder, Int. J. Heat Mass Transfer 35 (11) (1992) 3069–3075.
[16] K. Lundberg, W.C. Reynolds, W.M. Kays. Heat transfer with laminar flow in concentric annuli with constant and variable wall temperature and heat flux, Internal Report AHT-2, Dept. Mech. Eng., Stanford University, Stanford, CA, 1961.
[17] K. Lundberg, P.A. McCuen, W.C. Reynolds, Heat transfer in annular passages. Hydrodynamically developed laminar flow with arbitrarily prescribed wall temperatures or heat fluxes, Int. J. Heat Mass Transfer 6 (1963) 495–529.
[18] R.M. Manglik, P. Fang, Effect of eccentricity and thermal boundary conditions on laminar flow in annular ducts, Int. J. Heat Fluid Flow 16 (1995) 298–306.
[19] H. Moghadam, W. Aung, Numerical method for laminar convection in a concentric annular duct with vertical properties, Num. Heat Transfer A 18 (1990) 357–370.
[20] D.A. Nield, A.V. Kuznetsov, M. Xiong, Effects of viscous dissipation and flow work on forced convection in a channel filled by a saturated porous medium, Transport Porous Media 56 (2004) 351–367.
[21] P.J. Oliveira, F.T. Pinho, Axial annular flow of a nonlinear viscoelastic fluid—an analytical solution, J. Non-Newt. Fluid Mech. 93 (2000) 325–337.
[22] J.W. Ou, K.C. Cheng, Viscous dissipation effects on thermal entrance in laminar and turbulent pipe flows with uniform wall temperature, in: AIAA/ASME 1974 Thermophysics and Heat Transfer Conference, Boston, MA, 15–17 July 1974, Paper ASME 74-HT-50.
[23] W.C. Reynolds, K. Lundberg, P.A. McCuen, Heat transfer in annular passages—general formulation of the problem for arbitrarily prescribed wall temperatures or heat fluxes, Int. J. Heat Mass Transfer 5 (1963) 483.
[24] R.K. Shah, A.L. London, Laminar Flow Forced Convection in Ducts, Academic Press, New York, 1978.
[25] H.L. Toor, Heat transfer in forced convection with internal heat generation, AIChEJ 4 (3) (1958) 319–323.
[26] L.I. Urbanovich, Temperature distribution and heat transfer in a laminar incompressible annular channel flow with energy dissipation, J. Eng. Phys. Thermophys. 14 (4) (1968) 402–403.